

# The Effect of Electrolyte Concentration on the Chemical Force Titration Behavior of $\omega$ -Functionalized SAMs: Evidence for the Formation of Strong Ionic Hydrogen Bonds

D. Alastair Smith\* and Mark L. Wallwork

Department of Physics and Astronomy, University of Leeds, Leeds, U.K.

Jin Zhang, Jennifer Kirkham, and Colin Robinson

Division of Oral Biology, Leeds Dental Institute, Leeds, U.K.

Andrew Marsh and Michael Wong

Department of Chemistry, University of Warwick, Coventry, U.K.

Received: June 27, 2000

The chemical force titration behavior of carboxylic and phosphonic acid-functionalized tips and substrates has been found to be very strongly dependent on electrolyte concentration. Under low electrolyte concentration conditions, these force titrations take the form of peaks, which change to monotonic sigmoidal curves with a concomitant shift to lower pH as the electrolyte concentration of the buffer is increased. The appearance of a peak in the low electrolyte concentration force titrations is attributed to the formation of strong hydrogen bonds between neutral and ionized species on the tip and substrate, which is prevented in the case of high electrolyte concentration by the formation of an electric double layer. There is strong evidence that the measured  $pK_{1/2}$  (which corresponds to the pH of the bulk solution at which half of the surface groups are ionized) of these acid groups lies at the position of the peak of the low electrolyte concentration titration curves (carboxylic acid,  $pK_a = 8$ ; phosphonic acid,  $pK_{a1} = 4.6$ ,  $pK_{a2} = 8.4$ ) and cannot be measured under high electrolyte concentration conditions by this adhesion method. JKR theory of contact mechanics cannot be used to describe the low electrolyte concentration force titration data of these acid SAMs. The shapes of the force titration curves are described very well at all electrolyte concentrations by a simple model in which strong ionic and weak neutral hydrogen bonds contribute to the total adhesion force, which strongly supports our hypothesis. The results of fitting the force titration data to this model indicate that the strong ionic hydrogen bonds are on the order of 16 times stronger than a neutral hydrogen bond, which agrees well with theoretical predictions.

## Introduction

Intermolecular forces at surfaces on the micro- and nanometer scale are central to a wide range of biological, chemical, and physical processes (e.g., heterogeneous catalysis, colloidal chemistry, adhesives, lubrication, membrane transport, molecular recognition, cell signaling, and the control of a range of biochemical processes). Interactions that play a major role in controlling these phenomena include van der Waals forces, hydrogen bonding, and electrostatic charge interactions.<sup>1</sup>

A key feature of the chemistry of surfaces is the difference in the behavior of ionizable groups resident on those surfaces compared with their behavior free in solution. Although surface-specific techniques such as contact angle measurements<sup>1</sup> are able to probe the surface  $pK_a$  values of ionizable groups, the measurements are difficult to make if the surfaces are highly hydrophilic. The actual surface  $pK_a$  is not obtained by this technique, as it is the pH of the bulk solution that is, in fact, being measured. In addition, it would be of significant value in many applications to be able to map the surface energy,  $pK_a$ , and charge with high spatial resolution. The development of local probe techniques such as atomic force microscopy (AFM)

during the past 10 years has created new possibilities for the study of interfacial phenomena with resolution close to the atomic level.

The pioneering work of Ducker et al.<sup>2</sup> demonstrated that AFM could be used to probe the colloidal forces between two surfaces. In those experiments, the forces between a 7- $\mu\text{m}$  silica sphere and a flat silica surface were measured by gluing the silica sphere to an AFM cantilever. The approach curves were analyzed under varying conditions of solution pH and electrolyte concentration using the Derjaguin–Landau–Verwey–Overbeek<sup>1,3,4</sup> (DLVO) model of electric double layer forces. More recently, “chemical force microscopy” (CFM) has been introduced as a new mode of operation in which the AFM tips are chemically modified to have a specific functionality by the covalent attachment of a molecular monolayer using thiol self-assembly.<sup>5–11</sup> An extension of this technique, “force titration”, in which the tip–sample adhesion is monitored as a function of pH,<sup>11–16</sup> can be used to determine and map the  $pK_a$  of surface-bound groups with nanometer resolution.

The first examples of chemical force titrations were performed using carboxylic acid functionalized tips and samples at high ionic strength by Lieber<sup>15</sup> ( $10^{-2}$  M) and at lower ionic strength by Liu<sup>13</sup> ( $10^{-4}$  M). Lieber reported a *sigmoidal step* in the force titration curve that yielded an apparent  $pK_a$  of 5.5, approximately 0.75 pH units higher than the solution value.<sup>17</sup> Liu, on the other

\* Author to whom correspondence should be addressed: Dr. D. A. Smith, Department of Physics and Astronomy, University of Leeds, Leeds LS2 9JT, U.K. E-mail: d.a.m.smith@leeds.ac.uk.

hand, described a force titration curve that took the form of a *single peak* at pH 5 that was taken to represent the  $pK_a$ .

Other methods have been used to determine the surface  $pK_a$  of surface-confined carboxylic acid groups. In sharp contrast to the force titration results, Hu and Bard<sup>18</sup> used the method of Ducker<sup>2</sup> under ionic strength conditions intermediate between the previous two studies ( $10^{-3}$  M) and obtained a surface  $pK_a$  of 8, 3.25 units higher than the bulk aqueous value. Also, Godinez<sup>19</sup> used the pH dependence of the cathodic peak current in a voltammetric measurement at an ionic strength of  $10^{-1}$  M to obtain a  $pK_a$  for this group of 8, and Bain et al.<sup>20</sup> have reported measurements on carboxylic acid SAMs at high ionic strength that agree with this value. Clearly, there is a significant disparity in the observed force titration behavior and the measured  $pK_a$  of surface-bound carboxylic acids obtained using the various methods outlined above, and no satisfactory explanation has been given.

We have encountered widely varying force titration behavior depending on experimental parameters such as the ionic strength of the buffer solution and the length of the alkyl spacer unit of the  $\omega$ -functionalized alkanethiols. To elucidate these incongruities in a field that has recently generated great interest, we have made a systematic study of the chemical force titrations of carboxylic and phosphonic acid functional tips and substrates over a wide range of ionic strengths from  $\sim 10^{-7}$  to  $10^{-1}$  M. In this contribution, we show that the chemical force titration can take the form of a peak or a step depending on the ionic strength and that, under high ionic strength, the surface  $pK_a$  cannot be correctly obtained using AFM adhesion measurements. Only under low ionic strength can the surface  $pK_a$  be obtained, in which case it occurs at the position of the peak of the force titration curve.

The model we have used to explain the force titration behavior incorporates the formation of strong ionic hydrogen bonds between tip and sample. Normal hydrogen bonds between neutral species have strengths of 1–3 kcal/mol, but when the  $pK_a$  of the two species involved is closely matched, an ionic hydrogen bond is proposed, and has been measured in some cases, to be many times stronger ( $>20$  kcal/mol).<sup>21–26</sup> For example, Sekikawa et al. recently used infrared spectroscopy to study charge-transfer effects in a strongly hydrogen-bonded potassium salt of a carboxylic acid,<sup>27</sup> and the strength of some ionic carboxylic acid group hydrogen bonds has been calculated by Meot-Ner et al. to be 28–30 kcal/mol.<sup>26</sup> Using a simple treatment to model our data, we estimate that ionic hydrogen bonds formed between the tip and sample in our experiments are on the order of 10–30 times stronger than hydrogen bonds formed between neutral carboxylic acid SAM surfaces.

Ionic hydrogen bonds are common in charged systems in the gas phase and in crystals;<sup>22–27</sup> however, their existence and possible role in other systems, such as in the binding pockets of enzymes, is a highly controversial topic.<sup>28–33</sup> Even a small increase in the dielectric constant from the gas-phase value greatly reduces the strength of charged hydrogen bonds,<sup>21–26</sup> and therefore, they are never observed in aqueous solutions. However, the phenomenon of solvent ordering between the AFM tip and sample is well-known,<sup>1,10,34–36</sup> and it has been shown that the tip pushes through these layers and excludes solvent upon contact.<sup>10,34–36</sup> Under these circumstances, the dielectric constant in the tip–sample interaction volume may be sufficiently low to permit the formation of the charged hydrogen bonds in our experiments. To our knowledge, these data are the first direct measurements of the strength of these bonds relative to a normal hydrogen bond in such a system.

We believe that our data provide evidence to support the controversial hypothesis that strong ionic hydrogen bonds can exist in biological systems, providing water is excluded from the interaction volume.

## Experimental Section

**Materials.** All solvents used were reagent grade or better (Sigma-Aldrich, Gillingham, U.K.). Constant-strength ionic buffer solutions of various pH values were prepared as previously described using doubly distilled water.<sup>15,18</sup> Briefly, two solutions at ionic strength 0.01 M were initially prepared:  $\text{KH}_2\text{PO}_4$  (solution A) and  $\text{Na}_2\text{HPO}_4$  (solution B). Low ionic strength solutions ( $10^{-4}$ – $10^{-7}$  M) were made by serial dilutions of A and B. Very low ionic strength solutions were used in preference to pure water around pH 7 because of the instability in the pH of water near the neutral value.<sup>37</sup> Low ionic strength buffer solutions in the pH range 2–5 were prepared from solution A with the pH adjusted by adding small quantities ( $\sim 5$ – $20$   $\mu\text{L}$  in 10 mL) of dilute  $10^{-2}$  M HCl. Low ionic strength buffer solutions in the intermediate pH range 5–9 were prepared from mixtures of A and B, with the final composition determining the pH, and those at high pH were prepared from solution B, which was adjusted with dilute NaOH. High ionic strength buffers ( $10^{-1}$  M) were prepared by the addition of  $10^{-1}$  M KCl to A and B, and the pH of each solution was determined by titrating with either dilute HCl, dilute NaOH, or by mixing the two solutions, A and B, as with the low ionic strength buffers. It should be noted that, at very low electrolyte concentrations, it is impossible to keep the ionic strength constant over the pH range. However, the very low concentration electrolyte used ( $\sim 10^{-7}$  M) contains a much lower concentration of buffer ions in the transition region (pH 5–9) than the high or low ionic strength solutions, and it is in this region that the effect of the electrolyte concentration is significant. To maintain accurate pH measurements, the pH was checked immediately before and after the experiment.

$\omega$ -functionalized alkanethiols were either obtained commercially [16-mercaptohexadecanoic acid, 11-mercaptoundecanoic acid, 3-mercaptopropanoic acid (Sigma-Aldrich, Gillingham, U.K.)] or synthesized in our laboratories (11-thioundecyl-1-phosphonic acid).<sup>38</sup>

**Preparation of Chemically Modified Substrates and AFM Probes.** Flat gold substrates were prepared using a template stripping method<sup>39</sup> on silicon. Briefly, a clean silicon wafer surface (cleaned in water, methanol, and dichloromethane and blown dry with nitrogen) was coated with 150 nm of gold by thermal evaporation (Edwards Auto 306) at pressures  $<2 \times 10^{-6}$  mbar. Epo-Tek 377 adhesive (Promatech, Cirencester, U.K.) was used to bond a clean glass slide to the gold-coated surface of the silicon wafer. Because no chromium adhesion layer is used between the silicon and the gold, it is relatively simple to peel off the silicon wafer after curing the adhesive, revealing the gold surface that was in intimate contact with the silicon (surface roughness of approximately 3 nm per square micron). Commercially available  $\text{Si}_3\text{N}_4$  AFM cantilevers (Digital Instruments, Cambridge, U.K.) were coated with 100 nm of gold using the same thermal evaporation procedure as above but with a 10-nm chromium adhesion layer.

The template stripped gold surfaces were immersed in  $10^{-1}$  M ethanol solutions of the alkanethiol materials and left for at least 2 h at room temperature. The gold-coated tips were cleaned in a similar manner and placed into the alkanethiol solutions for up to 12 h to ensure complete monolayer formation. After removal from the solution, both the substrates and tips were

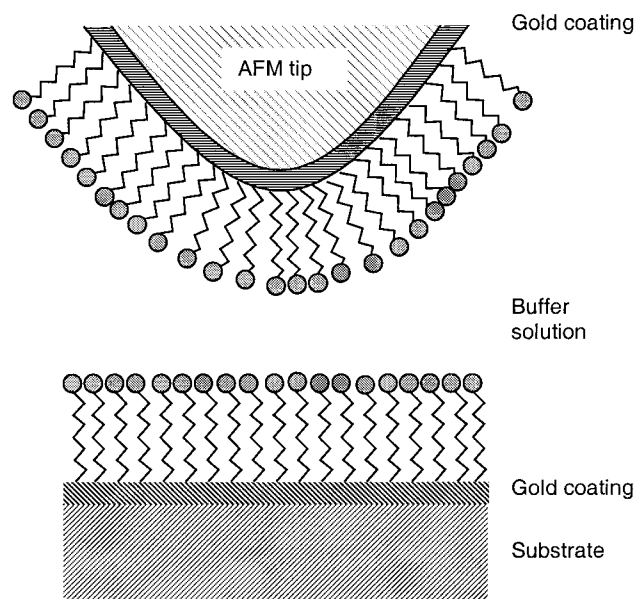


**Figure 1.** Experimental arrangement. An AFM tip and a flat substrate are coated with gold by thermal evaporation and modified with an  $\omega$ -functionalized alkanethiol self-assembled monolayer (SAM). This monolayer has a headgroup (shown as the solid circles) that provides the chemical functionality of the two surfaces that are brought into contact in buffer solution.

rinsed with ethanol and distilled water (pH 7) before being gently blown dry with nitrogen. Tips and substrates were then stored in a desiccator until use, which was no longer than 12 h after preparation and generally within 1 h. The quality of the SAMs was confirmed using contact angle, FTIR, and AFM measurements.

**Adhesion Measurements with AFM.** The standard experimental arrangement is shown in Figure 1. A modified tip is brought into contact with a modified substrate and then retracted. This approach–contact–retract cycle, or force–distance curve, is performed as a function of solution pH, and the data are referred to as a chemical force titration.<sup>11–16</sup> Force–distance curves and measurement of the adhesion forces were performed on a Molecular Imaging picoSPM (Molecular Imaging, Phoenix, AZ) controlled by Nanoscope IIIa electronics (Digital Instruments, Santa Barbara, CA) and Nanoscope software v 4.32. All force–distance curves were obtained under water or buffer solution in a Teflon fluid cell that was thoroughly cleaned and rinsed with methanol before use. With the tip and sample in place, the system was flushed with the appropriate buffer solution several times before the cell was finally filled and adhesion measurements were made.

The force–distance curves give the cantilever deflection versus sample displacement. Cycles of tip approach, contact, and retraction were recorded at a rate of 2 Hz with a  $z$  scan size on the order of 1  $\mu\text{m}$ . The point at which the tip separates from the sample on the retraction curve is known as the pull-off point. The difference between the pull-off point cantilever deflection and the point of zero deflection was converted to the adhesion force between the tip and sample using the cantilever spring constant, which was obtained from the Fourier transform of the thermal noise according to the method of Hutter et al.<sup>40</sup> The force constants for the gold-coated cantilevers determined by this method were on the order of 0.18–0.25 N/m after metalization. The tip radii were on the order of 50 nm and were checked with SEM before and after the experiments. Approximately 100 force–distance curves were obtained for

each pH value at several places on each sample within an area of about 2500 nm<sup>2</sup>.

It is important to note that adhesion titrations probe the interaction of the chemically modified tips and substrates as a function of the pH of the bulk solution, not the pH at the surface of the molecular monolayers. The pH at the surface,  $\text{pH}_s$ , is related to the bulk value,  $\text{pH}_\infty$ , by<sup>41,42</sup>

$$\text{pH}_s = \text{pH}_\infty + \frac{\psi}{2.303RT/F} \quad (1)$$

where  $\psi$  is the surface potential,  $R$  the ideal gas constant,  $T$  the absolute temperature, and  $F$  the Faraday constant. The  $\text{pK}_a$  of the surface groups,  $\text{pK}_a^{\text{surf}}$ , is related to the degree of ionization of the surface,  $\beta$ , and the solution  $\text{pH}_\infty$  by<sup>38,39</sup>

$$\log \frac{\beta}{1-\beta} = \text{pH}_\infty + \frac{\psi}{2.303RT/F} - \text{pK}_a^{\text{surf}} \quad (2)$$

The electrostatic surface potential is not measured by our adhesion experiments, and therefore, we define a quantity  $\text{pK}_{1/2}$  as the solution  $\text{pH}_\infty$  at which half of the groups are ionized and

$$\log \frac{\beta}{1-\beta} = \text{pH}_\infty - \text{pK}_{1/2} \quad (3)$$

The electrostatic term arising from the pH-dependent surface potential is generally on the order of 0.1–0.5 pH units,<sup>17</sup> and therefore, the quantity  $\text{pK}_{1/2}$ , which is the quantity reported by most groups,<sup>12–16</sup> is a relatively accurate measure of  $\text{pK}_a^{\text{surf}}$ .

SAMs terminated with carboxylic acid groups are known to form hydrogen bonds in the plane of the monolayer.<sup>43–45</sup> This effect has been shown to produce a shift in the IR-active carbonyl stretching mode toward lower energy.<sup>46</sup> This lateral hydrogen bonding makes deprotonation of the surface groups energetically less favorable, and in-plane hydrogen bonding will therefore affect the position of the surface  $\text{pK}_a$ .<sup>47,48</sup> Our experimental observable,  $\text{pK}_{1/2}$ , will therefore contain the effect not only of the surface potential but also of the in-plane hydrogen bonding; however, the current experiments do not allow us to quantify these contributions.

## Results and Discussion

### The Effect of Ionic Strength on the Force Titration Curves of Carboxylic Acid and Phosphonic Acid Groups. Carboxylic Acid Functionalized Tip and Substrate.

Figure 2 shows the chemical force titration curves acquired at three ionic strengths for tip and substrate both modified with 11-mercaptopundecanoic acid SAM. At very low ionic strength ( $\sim 10^{-7}$  M), the force titration takes the form of a single peak of approximately 60 nN centered at  $\text{pH} = 8$ . At low pH, a finite adhesion force of  $\sim 6$  nN is observed, and at  $\text{pH} > 12$ , almost zero adhesion is measured. At intermediate ( $10^{-4}$  M) and high ( $10^{-1}$  M) ionic strengths, the same adhesion forces are observed as at low pH, but the transition to zero adhesion occurs at pH values much lower than 12. The force titration peak decreases in size and shifts to lower pH with increasing ionic strength, until at  $10^{-1}$  M, no peak is observed, and the force titration curve is sigmoidal with a midpoint at about pH 5.

The adhesion behavior of the COOH surfaces at the two extremes of the pH scale is relatively easy to explain.<sup>13,15</sup> At low pH values around pH 2, the carboxylic acid groups on the tip and substrate will be fully protonated, and the finite adhesion force can be attributed to the formation of complementary hydrogen bonds between the two surfaces under all ionic strength conditions. Hydrogen bonding between neutral groups



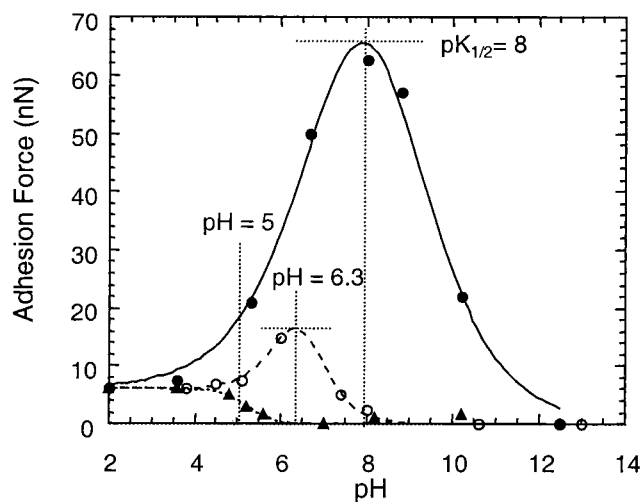


**Figure 2.** Chemical force titration curves for tip and substrate both modified with 11-mercaptoundecanoic acid SAMs acquired at three electrolyte concentrations: low electrolyte concentration ( $\sim 10^{-7}$  M, solid circles), intermediate electrolyte concentration ( $10^{-4}$  M, open circles), and high electrolyte concentration ( $10^{-1}$  M, solid triangles). (The curves have been added only as a guide to the eye.)

is almost unaffected by ionic strength, and an adhesion force of about 6 nN is measured in each case. At high pH values, when the surfaces are fully deprotonated, hydrogen bonds cannot form between the two surfaces, and zero adhesion is measured. The electrostatic repulsion (between the ionized groups on the tip and sample in the low ionic strength case and between two electric double layers under high ionic strength conditions) is clearly observed in the approach part of the force–distance curves (data not shown). Because our measurements are made in the retraction part of the curve and only adhesion forces are recorded, this repulsive electrostatic interaction is not quantified in our data. However, the experiments of Hu and Bard,<sup>18</sup> for example, are a direct probe of these long-range electrostatic forces, which, through calculation of the surface charge and potential, can be related to the fraction of ionized groups on the surface and the true surface  $pK_a^{\text{surf}}$  (eq 2).

When the interaction energy between two SAM-modified surfaces is considered, it is necessary to include the attractive van der Waals interaction between the two underlying metal surfaces, which is related to the Hamaker constants of the metals used. The van der Waals interaction between a sphere of radius  $R$  at a distance  $d$  from a planar substrate is given by<sup>1</sup>

$$\frac{F}{R} = -\frac{A_H}{6d^2} \quad (4)$$

where  $A_H$  is the Hamaker constant. For the gold–gold interaction, the Hamaker constants are quite large and have been measured to be on the order of  $25\text{--}40 \times 10^{-20}$  J in aqueous solutions.<sup>49,50</sup> Kane and Mulvaney<sup>51</sup> showed that the normalized adhesion force between a gold-coated tungsten sphere and a gold-coated substrate in ethanol was approximately 1 mN/m. However, after the introduction of 11-mercaptoundecanoic acid and the formation of SAMs on the two surfaces, there was a large reduction in the dispersion interaction by an order of magnitude. A similar effect on the approach curves of a silica sphere and a template-stripped gold surface in de-ionized water (pH 6.0) was also noted by Hu and Bard.<sup>18</sup> In this case, the dispersion interaction between silica and gold was also drastically reduced after the gold surface had been modified with 2-mercaptoundecanoic acid, a SAM that provides a much shorter

spacer length. It is therefore assumed in these discussions that the gold–gold interaction between our modified tip and substrate will only contribute a small component of the overall adhesion force because of the long spacer lengths of the SAMs involved.

Previous studies of the pull-off force between SAMs terminated with hydrophobic methyl groups<sup>52</sup> have shown that an increase in electrolyte concentration (NaCl, CaCl<sub>2</sub>, and Na<sub>2</sub>SO<sub>4</sub> were used in this case) from low concentration ( $10^{-4}$  M) to high concentration (1.5 M) caused an increase in the magnitude of the adhesion between the hydrophobic surfaces by as much as 50%. However, the wetting properties of the SAM, measured by contact angle experiments, were not affected, and it was concluded that the addition of electrolyte altered some property other than the affinity of the solvent for the surface. In that work, it was theorized that the reduction in the chemical potential of the water by the addition of the electrolyte caused the increase in pull-off force. In our experiments with hydrophilic surfaces at intermediate pH, the opposite effect was observed, i.e., as the electrolyte concentration was increased, the adhesive forces between tip and sample decreased (from 60 to 0 nN). The effect of osmotic pressure on the adhesion appears, therefore, to be negligible in our case, and the effects to be considered are hydrogen-bond formation and cation binding to the SAM surfaces.

The shape of the force titration curve at high ( $10^{-1}$  M) ionic strength has been discussed by Lieber.<sup>15</sup> The sigmoidal shape was modeled using the Johnson–Kendall–Roberts (JKR) theory of contact mechanics.<sup>1,53</sup> At high ionic strength, taking into account the effect of the electric double layer, JKR theory gives the surface  $pK_a$  as the pH at which the adhesion force is one-quarter of the way down the step between the fully protonated (maximum adhesion) and fully deprotonated (minimum adhesion) states. In the absence of an electric double layer, at very low ionic strength, JKR theory also predicts a steplike force titration but with the surface  $pK_a$  at a point halfway down the transition between maximum and minimum adhesion forces. Applying JKR theory to our high ionic strength data gives a surface  $pK_a$  of 4.9, in very good agreement with the result obtained by Lieber<sup>15</sup> and close to the value of the  $pK_a$  for the carboxyl group free in aqueous solution.<sup>17</sup> However, our data at intermediate ( $10^{-4}$  M) and very low ionic strengths ( $\sim 10^{-7}$  M) and those of Liu<sup>13</sup> at  $10^{-4}$  M deviate dramatically from the predictions of JKR theory and exhibit a peak in the force titration curve that shifts toward higher pH with decreasing ionic strength. These data bring into question the applicability of JKR theory for modeling AFM adhesion data, despite the fact that they appear to fit the high ionic strength data well.

The reason for the failure of JKR theory in these cases is principally the fact that it is a macroscopic theory of contact mechanics, not a model of microscopic adhesion. In JKR theory, the area of contact must be macroscopic (semi-infinite) so that the interfacial free energy is given by a single parameter,  $\gamma$ , appropriate for the surface materials. In the micro- or nanoscopic regime, specific molecular interactions (which do not rule out the use of JKR theory on macroscopic surfaces, because the work of adhesion is still correctly defined) make the approach unreliable. In addition, the measured adhesion between the modified AFM tip and substrate also depends on other factors that are very difficult to quantify, such as tip geometry, the competition between in-plane and out-of-plane interactions, the degree of solvent exclusion from the tip–sample volume, the interaction of buffer ions with the modified tips, and deformation of the molecular monolayer by the contact process. We must therefore consider a different model that can account for the

increase in adhesion force with increasing pH and the occurrence of a peak in the titration curve.

COOH SAM surfaces are known to contain significant degrees of in-plane hydrogen bonding between the carboxylic acid headgroups.<sup>43–45</sup> During the force–distance measurement, as the tip and sample make contact, it has been suggested that some of the in-plane hydrogen bonding must be destroyed and out-of-plane bonds formed between the two surfaces.<sup>13</sup> Within this picture of tip–sample hydrogen bonding, the occurrence of a peak in the force titration suggests that either (a) stronger out-of-plane bonds are being formed or (b) more of the normal out-of-plane bonds are formed as the surface is ionized. If the latter is true, then, according to our adhesion measurements, there must be an order of magnitude increase in the number of groups available for hydrogen bonding between the tip and sample at the pH corresponding to the peak of the curve than at low pH. It is difficult to envisage how the conformation of the SAM surface could be so drastically altered to provide this 10-fold increase in groups available for hydrogen bonding, and in fact, the chemical force titration of the phosphonic acid SAM surfaces, discussed below, appears to confirm that the peak does not arise from an increase in the number of hydrogen bonds formed.

**Phosphonic Acid Functionalized Tip and Substrate.** The synthesis and characterization of a PO(OH)<sub>2</sub>-terminated SAM have been described previously, and preliminary discussions of the force titration were presented.<sup>38</sup> Briefly, force titrations were performed at the two extremes of ionic strength, 10<sup>-1</sup> and 10<sup>-4</sup> M. Under very low ionic strength conditions (10<sup>-4</sup> M, Figure 3a), the force titration curve exhibits two peaks at pH 4.6 and 8.4, corresponding to the ionization of the two hydroxyl groups of this diprotic acid. Behavior similar to that of the carboxylic acid SAMs is observed when conditions are changed to high ionic strength (10<sup>-1</sup> M, Figure 3b), where the peaks are replaced by shoulders with an accompanying shift of the midpoints to lower pH (4.6 and 7.7, respectively).

Changing the electrolyte concentration, therefore, appears to have the same effect on the form of the force titration of the phosphonic acid SAM as was observed for the carboxylic acid functionality. In the case of this phosphonic acid SAM, one of the hydroxyl groups lies in the plane of the monolayer and takes part in intramonolayer hydrogen bonding, and the other lies out of the plane of the SAM.<sup>38</sup> If the peaks in these force titrations at low ionic strength are due to the formation of *more* hydrogen bonds (perhaps permitted by a conformational change in the SAM structure), then we would expect to see a difference between the two force titration features obtained for the phosphonic acid SAM. This is because one group is involved in in-plane hydrogen bonding (as with the carboxylic acid SAM) and the other lies out of the plane of the monolayer. The number of out-of-plane groups, which are available for interaction between the tip and substrate, cannot be increased, and yet the two groups of this diprotic acid SAM both produce a peak in the low ionic strength force titration and exhibit exactly the same response to an increase in the ionic strength. Therefore, we must conclude that a *stronger* interaction occurs between tip and substrate as the pH is increased at low ionic strength, which results in the formation of the observed peaks.

Hydrogen bonds formed between ionized and neutral acid groups are stronger because of their increased ionic character.<sup>21–26</sup> An extreme example is the HCOOH...<sup>-</sup>F hydrogen bond of 60 kcal/mol, compared with a normal “weak” hydrogen bond of a few kilocalories per mole.<sup>54,55</sup> The anionic HCOOH...<sup>-</sup>OOC is predicted and has been measured in the gas phase to have a

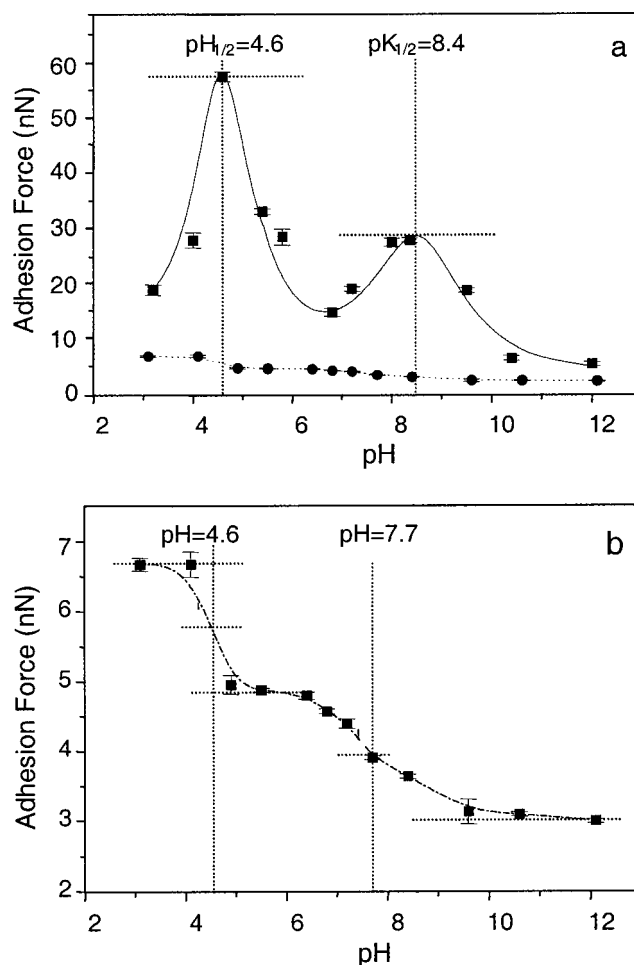


**Figure 3.** Chemical force titration curves for tip and substrate modified with an 11-thioundecyl-1-phosphonic acid SAMs. (a) Titration performed in high (10<sup>-1</sup> M, solid circles) and low (10<sup>-7</sup> M, solid squares) electrolyte concentration solutions and (b) expanded view of the high electrolyte concentration data.

strength of 28–30 kcal/mol.<sup>26</sup> Recently, Shan et al.<sup>56</sup> investigated hydrogen-bond strengths as a function of the difference in pK<sub>a</sub> of the donor and acceptor groups and found that, when the pK<sub>a</sub>s are matched, the maximum bond strength is achieved. These short, strong hydrogen bonds only exist in low dielectric constant media, and small increases in dielectric constant rapidly reduce their strength;<sup>22–26</sup> consequently, one would initially rule out a possible role in AFM adhesion measurements in aqueous solution.

However, it has been shown that solvent is expelled from the interaction volume when the tip and sample are brought into contact.<sup>10,34–36</sup> The hydration force between a conical tip with a spherical apex and a flat specimen surface at separation distances on the order of 1 water molecule has been calculated to be on the order of ~0.5 nN.<sup>57</sup> These calculations were performed for a tip of low radius of curvature (~4 nm). For tips with a radius of ~50 nm as used in these experiments, a hydration force between tip and sample of approximately 4 nN is calculated at a tip–sample separation corresponding to the final water layer. The applied force in our experiments is generally higher than this (>10 nN), and furthermore, tip asperities may lead to a lower applied force before the last water layer is removed.<sup>57</sup> We can therefore assume that the two SAM surfaces come into contact, with the displacement of the last remaining water molecule. (The threshold load for damage to a SAM has been found to be in the region 300 nN,<sup>58</sup> and

therefore, it is highly unlikely that the SAMs are damaged by our experiments; indeed, there is a very high degree of reproducibility in the measurements.) The removal of water from the interaction volume is assisted by the hydrogen-bonding properties of the COOH headgroups. Meot-ner et al.<sup>26</sup> have shown that, in concentrated solutions, carboxylic acid groups tend to hydrogen bond to each other and carboxylate anions with a concomitant displacement of water.

The dielectric constant in the tip-sample interaction region will therefore be considerably lower than that of bulk water, perhaps close to the value for a short chain acid or alkyl chain (propanoic acid,  $\epsilon = 3.4$ ; butanoic acid,  $\epsilon = 2.98$ ; long alkyl chains,  $\epsilon \approx 1.5$ ), and may well be low enough to permit the formation of strong ionic hydrogen bonds. We therefore propose that, as the pH increases and the surface groups ionize, strong  $\text{COO}^- \cdots \text{HOOC}$  bonds can form between tip and sample and that these bonds increase the measured adhesion force, which leads to a peak in the force titration curve. At the  $\text{p}K_{1/2}$ , when half of the groups on the substrate are ionized, the maximum adhesion force is obtained. Above the  $\text{p}K_{1/2}$ , the adhesion force then decreases because, when more than half of the surface groups are ionized, the number of neutral acid groups available in the surface, which are required to form the strong hydrogen-bond pairs, decreases. Our low electrolyte concentration data indicate that the  $\text{p}K_{1/2}$  of the carboxylic acid group is pH 8, in very good agreement with the  $\text{p}K_{\text{a}}^{\text{surf}}$  values obtained from approach curve data at  $10^{-1}$  M by Hu and Bard<sup>18</sup> and with the results of Godinez<sup>19</sup> obtained from cyclic voltammetry at  $10^{-1}$  M.

The effect of changing the ionic strength on the  $\text{p}K_{\text{a}}$  of groups *in solution* is typically to shift the value by a small fraction of 1 pH unit. However, the  $\text{p}K_{1/2}$  measured by AFM adhesion appears to be a strong function of electrolyte concentration (the low electrolyte concentration peak is shifted by 3 units to higher pH in comparison with the midpoint of the high electrolyte concentration step). However, we suggest that the step does not occur at, or near, the  $\text{p}K_{\text{a}}^{\text{surf}}$ . The shift in the peak can be accounted for by the association of buffer counterions with the ionized groups in the SAM and the effect this has on the formation of intra- and intermonolayer  $\text{COO}^- \cdots \text{HO}$  bonds. As has been mentioned, neutral COOH SAM surfaces are known to contain significant degrees of in-plane hydrogen bonding,<sup>43–45</sup> and it seems likely that, at low degrees of ionization, the ionized species also take part in hydrogen bonding within the plane of the monolayer in the absence of buffer counterions. The formation of these strong in-plane bonds would make it more difficult to deprotonate the neutral species that are involved,<sup>12,18,59</sup> and thus, the  $\text{p}K_{1/2}$  is shifted to higher pH. At higher electrolyte concentration, these strong in-plane bonds are prevented from forming by the formation of ion pairs between the deprotonated acid groups and buffer cations, and the remaining neutral groups in the surface can be ionized at a lower pH. In addition, the ionic radii of the buffer cations are comparable to the hydrogen-bond length,<sup>17,21</sup> and therefore, only a small fraction of the SAM surface need be ionized before the association of buffer ions hinders the formation of out-of-plane ionic hydrogen bonds between tip and substrate. Thus, the adhesion force drops rapidly to zero at a pH well below the actual  $\text{p}K_{\text{a}}^{\text{surf}}$ , increasing the observed shift between the high and low electrolyte concentration force titration curves.

The surface  $\text{p}K_{1/2}$  or the  $\text{p}K_{\text{a}}^{\text{surf}}$  cannot be measured accurately by applying JKR theory to AFM adhesion force measurements at any electrolyte concentration, and only in very low electrolyte concentration conditions can adhesion force data provide an

accurate surface  $\text{p}K_{1/2}$  from the position of the peak in the force titration curve.

The form of the phosphonic acid force titration curves and their dependence on electrolyte concentration can also be explained using this framework. Under low electrolyte concentration conditions, the peaks in the curve arise because of the formation of strong, ionic out-of-plane hydrogen bonds between neutral and charged species on the tip and substrate. In the high electrolyte concentration buffer, the formation of an electric double layer prevents the strong ionic hydrogen bonding both in the monolayer and between the two monolayers, and the adhesion force falls monotonically.

The carboxylic acid force titrations shows a shift of 3 pH units between the peak at low electrolyte concentration and the midpoint of the step at high electrolyte concentration because of the formation of strong, in-plane ionic hydrogen bonds that stabilize the neutral species and increase the  $\text{p}K_{1/2}$ . In the case of the phosphonic acid, the peak and step at higher pH are also shifted with respect to each other (by  $\sim 0.7$  pH units) for the same reason, as this hydroxyl group lies in the plane of the monolayer and is involved in intramonolayer bonding. The midpoint of the lower pH step and peak occur at the same pH ( $\sim 4.6$ ), which suggests that the  $\text{p}K_{1/2}$  of this group is unaffected by electrolyte concentration, which is in accord with our picture of this group lying out of the plane of the monolayer and not forming in-plane hydrogen bonds.

*A Simple Model for the Force Titration Curves of Hydrogen-Bonding Surfaces.* Attempts to model the shape of the low electrolyte concentration force titration curves using intermonolayer hydrogen bonding and electrostatic repulsion between two charged surfaces were completely unsuccessful. However, a very simple model based on the proposed formation of two types of hydrogen bond, strong and weak, can be developed. The forces required to rupture one neutral (weak) and one ionic (strong) hydrogen bond can be represented by  $f_{\text{hb}}$  and  $f_{\text{HB}}$  respectively, and the ionic bond can be assumed to be stronger by a factor of  $m$ , i.e.,  $f_{\text{HB}} = mf_{\text{hb}}$ . Denoting the fraction of ionized groups in the surfaces by  $\beta$  and the total number of groups in the contact area by  $2N$  (i.e.,  $N$  on each surface), then the total number of ionized groups within the contact area is  $2\beta N$ . The fraction of these groups that form ionic hydrogen bonds with neutral groups when the tip and substrate come together is  $2\beta(1 - \beta)$ , and assuming that all of these form a bond, then the total number of strong bonds formed is given by  $2N\beta(1 - \beta)$ . The number of neutral hydrogen bonds that can be formed is given by  $N(1 - \beta)(1 - \beta)$  (the factor 2 is missing because these bonds involve neutral groups on both surfaces). Therefore, the total adhesion force due to hydrogen-bond formation,  $F_{\text{T}}$ , can be expressed as a simple sum of these two interactions

$$F_{\text{T}} = 2N(1 - \beta)\beta f_{\text{HB}} + N(1 - \beta)(1 - \beta)f_{\text{hb}} \quad (5)$$

which can be rewritten as

$$F_{\text{T}} = Nf_{\text{hb}}[2(1 - \beta)\beta m + (1 - \beta)(1 - \beta)] \quad (6)$$

Now, the force titration curves are acquired as a function of  $\text{pH}_{\infty}$  of the bulk solution, not as a function of  $\beta$ , the degree of surface ionization. The measured  $\text{p}K_{1/2}$  (which is the *solution*  $\text{pH}_{\infty}$  at which half of the groups are ionized), is related to  $\beta$  by eq 3, and so the total adhesion force can be rewritten in terms of the variable  $\alpha = \text{pH}_{\infty} - \text{p}K_{1/2}$  as

$$F_{\text{T}} = Nf_{\text{hb}} \left[ m \frac{2 \cdot 10^{\alpha}}{(1 + 10^{\alpha})^2} + \frac{1}{(1 + 10^{\alpha})^2} \right] \quad (7)$$



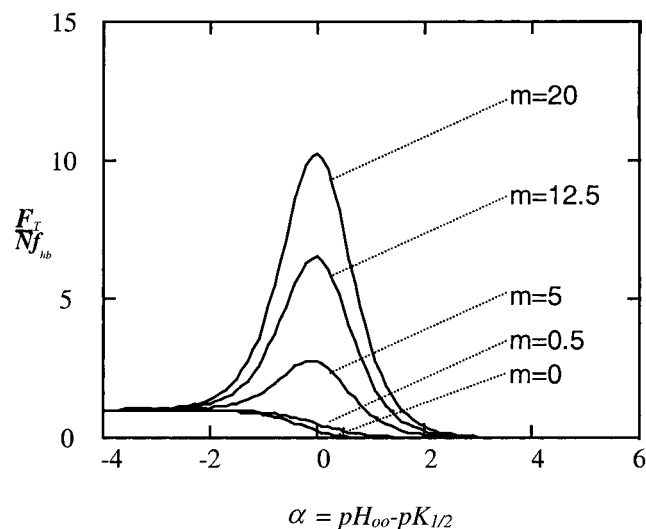


**Figure 4.** The total adhesion titration can be modeled as a linear combination of strong ionic and weak neutral hydrogen bonds. The theoretical force titrations produced by this model are plotted for different values of  $m$ , the ratio of the strength of these two bonds, and normalized to the product of the number of interacting groups and the strength of a neutral weak hydrogen bond,  $N_{f_{hb}}$ .  $pH_{00}$  is the pH of the bulk solution, and  $pK_{1/2}$  is defined as the pH at which half of the surface groups are ionized (see eq 3). The shape of the low electrolyte concentration curves are reproduced by values of  $m \approx 15-20$ , whereas the high electrolyte concentration sigmoidal step is reproduced by  $m = 0$ , i.e., no strong hydrogen bonds formed [caused by the interaction of buffer ions with the ionized acid groups in the SAMs (see discussion)].

Although it is possible to make a very good estimate of the number of carboxylic acid groups in the contact area and the strength of a single neutral hydrogen bond, there are a number of important factors that affect the magnitude of  $F_T$  that are very difficult to quantify. For example, these include the effect of tip geometry and the competition between the formation of out-of-plane and in-plane hydrogen bonding. In addition, the rate at which the approach-retract cycle is performed also affects the total adhesion force measured.<sup>60</sup> It is therefore not possible to plot absolute force versus  $\alpha$  accurately, so  $F_T$  is normalized to  $N_{f_{hb}}$ , and this quantity is plotted in Figure 4.

Although this model is rather crude, it accurately reproduces the shape of the force titrations and the transition from a peak to a step by reducing the contribution of the strong ionic hydrogen bonds. It also yields values of  $m \approx 15-20$  when the low electrolyte concentration experimental data are fit, which is in excellent agreement with theoretical predictions.<sup>21-27</sup> However, the model does not fit the width of the transition at all well. At low electrolyte concentration, the peak width in Figure 2 is approximately twice that predicted by the model. It is well-known that, as the length of the alkyl spacer linking the carboxylic acid to the gold substrate through the thiol-gold bond is increased, the alkyl chains pack to form a more crystalline structure and a more ordered monolayer.<sup>9</sup> Shorter alkyl chains are more fluid, and considerable disorder is present in short spacer SAMs. In Figure 2, the data have been obtained from a SAM with an 11-carbon-chain spacer, which would be expected to produce a SAM with some disorder.<sup>9</sup> Therefore, a possible reason for the observed transition being wider than predicted by the model is that disorder in the SAM surface results in a heterogeneity in headgroup environments and, therefore, a wider distribution of  $pK_a$  values than would be expected in a perfectly crystalline, homogeneous monolayer. To test this hypothesis, we performed a series of experiments

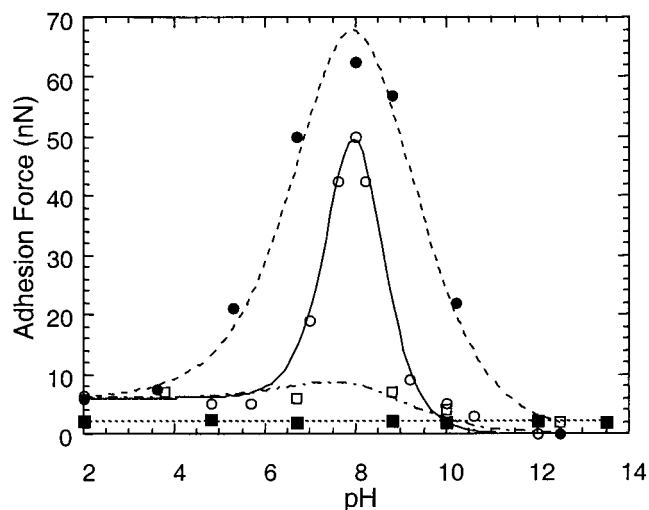


**Figure 5.** Chemical force titration curves in very low electrolyte concentration buffer ( $10^{-7}$  M) for (a) tip and substrate both modified with 16-mercaptohexadecanoic acid on gold (16:16, open circles), (b) tip and substrate both modified with 11-mercaptoundecanoic acid on gold (11:11, solid circles), (c) tip modified with 11-mercaptoundecanoic acid and substrate modified with 3-mercaptopropanoic acid (11:3, open squares), and (d) tip and substrate both modified with 3-mercaptopropanoic acid (3:3, solid squares). The simple model of Figure 4 reproduces the shape of the titration curves but not the width of any but the longest alkyl spacer monolayers because of disorder in the shorter alkyl spacer SAMs. (Curves through the 11:11, 11:3, and 3:3 data are only a guide to the eye, but the 16:16 peak is accurately fit by eq 6, yielding a value of  $m \approx 16$ ).

with SAMs of varying alkyl spacer length on tips and substrates in very low electrolyte concentration solutions.

Chemical force titrations of the carboxylic acid headgroup were performed using combinations on tip and substrate of alkyl chains comprising 16, 11, and 3 carbons, namely 16:16, 11:11, 11:3, and 3:3 on tip and sample, respectively. The results are shown in Figure 5. (The 11:11 data are reproduced from Figure 2.) The force titrations (except for the combination of shortest spacer length, 3:3) exhibit a single peak centered at about pH 8, independent of chain length. The magnitude of the maximum adhesion force decreases with decreasing spacer length until no peak is observed in the case when both tip and substrate are modified with 3-carbon-chain SAMs. In the case of the 11:11, 11:3, and 3:3 force titrations, the curves in Figure 5 are simply added as a guide to the eye and are not fit using the model. The 16:16 carbon spacer SAM force titration is much narrower than the 11:11 curve, and the width of this transition is accurately reproduced by our model which was used to fit the 16:16 data in Figure 5. This SAM is more ordered,<sup>9</sup> and it therefore appears that the increase in width of the 11:11 SAM force titration feature is indeed due to the increased disorder in this system. The slightly lower peak adhesion force that is measured in the 16:16 system is also probably due to the more highly ordered SAM exhibiting higher degrees of in-plane hydrogen bonding, which competes with the intermonolayer bonding when the surfaces contact. Using the model to fit 16:16 carbon spacer carboxylic acid force titration data yields a  $pK_{1/2}$  of 8 and a value of  $m$ , the factor by which the ionic hydrogen bonds are stronger than the neutral ones, of 16, which is in excellent agreement with theoretical predictions and gas-phase measurements.<sup>21-27</sup>

The 2-nN adhesion force observed with the shortest carbon spacer SAMs (3:3), which is independent of pH, arises from the interaction of two surfaces in which both the hydrophilic, hydrogen-bonding carboxylic acid headgroups and the hydro-

phobic alkyl chains are exposed, i.e., a mixed hydrophilic/hydrophobic interaction. This was confirmed by performing the force titration with a more ordered hydrophobic tip and hydrophilic substrate (an 11-mercaptoundecane tip and an 11-mercapoundecanoic acid substrate). An identical 2-nN adhesion force, which was independent of pH, was also observed (data not shown).

## Conclusions

The chemical force titration behavior of carboxylic and phosphonic acid functionalized tips and substrates has been found to be very strongly dependent on electrolyte concentration. The carboxylic acid force titration exhibits a single peak at very low electrolyte concentration and a sigmoidal curve under high electrolyte concentration conditions. The formation of a peak in the force titration at very low electrolyte concentration could be due to the formation of more hydrogen bonds between tip and sample with increasing pH or to an increase in the strength of the interaction. The behavior of the phosphonic acid titration, which exhibits two peaks in the force titration due to the presence of two ionizable OH groups, strongly supports the latter argument. This is because one of the OH groups lies in the plane of the monolayer, as with the carboxylic acid SAM, but the other lies out-of-plane. Both of these OH groups show the transition from a peak to a sigmoidal force titration as the electrolyte concentration is increased, and therefore, because one group is out of the plane of the monolayer, it is extremely unlikely that the number of groups involved in hydrogen bonding between tip and substrate could be increased.

The appearance of a peak in these force titrations is attributed to the formation of strong hydrogen bonding between neutral and ionized species on the tip and substrate, which is prevented in the case of high electrolyte concentration by the formation of an electric double layer.

There is strong evidence that the measured  $pK_{1/2}$  (which corresponds to the pH of the bulk solution when half the surface groups are ionized) of these acid groups lies at the peak of the very low electrolyte concentration titration curves (carboxylic acid,  $pK_a = 8$ ; phosphonic acid,  $pK_{a1} = 4.6$ ,  $pK_{a2} = 8.4$ ), which is in good agreement with the  $pK_a^{surf}$  measured by other techniques not involving adhesion or contact. We are forced to conclude that the  $pK_{1/2}$  cannot be measured under high electrolyte concentration conditions by adhesion. A JKR contact mechanics treatment of the titrations cannot account for the shape of the low electrolyte concentration data nor does it yield an accurate value of  $pK_{1/2}$  when applied to the high electrolyte concentration data. The sigmoidal form of the high electrolyte concentration data is coincidentally what would be predicted by JKR theory but is, in fact, due to the electric double layer preventing the formation of strong, ionic hydrogen bonds between tip and substrate. This association of ions with ionized groups in the SAM also has the effect of preventing in-plane ionic hydrogen bonding, which further serves to push the sigmoidal midpoint to lower pH in comparison with the peak under low electrolyte concentration conditions.

The shapes of the force titration curves of the carboxylic and phosphonic acid SAMs at all electrolyte concentrations are effectively described by a simple model in which strong ionic and weak neutral hydrogen bonds contribute to the total adhesion force. The effect of SAM disorder on the low electrolyte concentration titration curve has been investigated by using SAMs with varying alkyl spacer lengths, and it has been observed that disorder causes the peak to broaden so that the simple model is unable to fit the transition width in these SAMs.

Well-ordered SAMs with long (16-carbon) alkyl spacers produce a much narrower force titration peak, which is fit very well by the model. The results of fitting this SAM force titration data indicate that the strong ionic hydrogen bonds are on the order of 16 times stronger than a neutral hydrogen bond, which agrees well with both theoretical predictions and experimental measurements in the gaseous and solid phases.

To our knowledge, our data are the first example of measurements of the relative strength of strong hydrogen bonds in such a system in which the water is expelled from the interaction volume, thus reducing the local dielectric constant to a value close to 1, which is necessary for these strong bonds to form. It has been suggested, and has caused much controversy, that these strong bonds are important in enzyme catalysis and other biological interactions. Our data suggest that this hypothesis could be true if water is expelled from the enzyme active site when the substrate binds.

**Acknowledgment.** The authors thank the BBSRC (Grant 24/9709001) and the Leeds General Infirmary National Health Service Trust for financial support.

## References and Notes

- (1) Israelachvili, J. *Intermolecular and Surface Forces*, 2nd ed.; Academic Press: London, 1992.
- (2) Ducker, W. A.; Senden, T. J.; Pashley, R. M. *Nature* **1991**, *353*, 239–241.
- (3) Derjaguin, B. V.; Landau, L. *Acta Physicochim. URSS* **1941**, 633–662.
- (4) Verwey, E. J. W.; Overbeek, J. Th. G. *Theory of Stability of Lyophobic Colloids*; Elsevier: Amsterdam, 1948.
- (5) Frisbie, C. D.; Rozsnyai, L. F.; Noy, A.; Wrighton, M. S.; Lieber, C. M. *Science* **1994**, *265*, 2071–2074.
- (6) Noy, A.; Frisbie, C. D.; Rozsnyai, L. F.; Wrighton, M. S.; Lieber, C. M. *J. Am. Chem. Soc.* **1995**, *117*, 7943–7951.
- (7) Green, J.-B. D.; McDermott, M. T.; Porter, M. D.; Siperko, L. M. *J. Phys. Chem.* **1995**, *99*, 10960–10965.
- (8) Ito, T.; Namba, M.; Buhlmann, P.; Umezawa, Y. *Langmuir* **1997**, *13*, 4323–4332.
- (9) Ulman, A. *An Introduction to Ultrathin Organic Films: From Langmuir-Blodgett to Self-Assembly*; Academic Press: San Diego, CA, 1991.
- (10) Sinniah, S. K.; Steel, A. B.; Miller, C. J.; Rett-Robey, J. E. *J. Am. Chem. Soc.* **1996**, *118*, 8925–8931.
- (11) Takano, H.; Kenseth, J. R.; Wong, S.-S.; O'Brien, J. C.; Porter, M. D. *Chem. Rev.* **1999**, *99*, 2845–2890.
- (12) van der Vegte, E. W.; Hadziannou, G. *J. Phys. Chem. B* **1997**, *101*, 9563–9569.
- (13) He, H. X.; Li, C. Z.; Song, J. Q.; Mu, T.; Wang, L.; Zhang, H. L.; Liu, Z. F. *Mol. Cryst. Liq. Cryst.* **1997**, *99*, A294–295.
- (14) Zhang, H.; He, H. X.; Wang, J.; Mu, T.; Liu, Z. F. *Appl. Phys.* **1998**, *A66*, S269–271.
- (15) Vezenov, D. V.; Noy, A.; Rozsnyai, L. F.; Lieber, C. M. *J. Am. Chem. Soc.* **1997**, *119*, 2006–2015.
- (16) Zhang, H.; He, H. X.; Mu, T.; Liu, Z. F. *Thin Solid Films* **1998b**, *778*, 327–329.
- (17) Lide, D. R. *CRC Handbook of Chemistry and Physics*, 72nd ed.; Boca Raton, FL, 1991.
- (18) Hu, K.; Bard, A. J. *Langmuir* **1997**, *13*, 5114–5119.
- (19) Godinez, L. A.; Castro, R.; Kaifer, A. E. *Langmuir* **1996**, *12*, 5087–5092.
- (20) Bain, C. D.; Whitesides, G. M. *Langmuir* **1989**, *5*, 1370–1376.
- (21) Hadzi, D., Ed. *Theoretical Treatments of Hydrogen Bonding*; Wiley: Chichester, U.K., 1997.
- (22) Cleland, W. W.; Kreevoy, M. M. *Science* **1991**, *264*, 1887–1890.
- (23) Chen, J.; McAllister, M. A.; Lee, J. K.; Houk, K. N. *J. Org. Chem.* **1998**, *63*, 4611–4619.
- (24) Meot-ner, M.; Sieck, L. W. *J. Phys. Chem.* **1986**, *90*, 6687–6692.
- (25) Stahl, N.; Jencks, W. P. *J. Am. Chem. Soc.* **1986**, *108*, 4196–4203.
- (26) Meot-ner, M.; Elmore, D. E.; Scheiner, S. *J. Am. Chem. Soc.* **1999**, *121*, 7625–7635.
- (27) Sekikawa, T.; Miyakubo, K.; Takeda, S.; Kobayashi, T. *J. Phys. Chem.* **1996**, *100*, 5844–5848.
- (28) Gerlt, J. A.; Gassman, P. G. *Biochemistry* **1993**, *32*, 11943–11952.
- (29) Frey, P. A.; Whitt, S. A.; Tobin, J. B. *Science* **1994**, *264*, 1927–1933.



- (30) Scheiner, S.; Kar, T. *J. Am. Chem. Soc.* **1995**, *117*, 6970–6975.
- (31) Shan, S. O.; Herschlag, D. *J. Am. Chem. Soc.* **1996**, *118*, 5515–5518.
- (32) Shan, S. O.; Herschlag, D. *Proc. Natl. Acad. Sci. U.S.A.* **1996**, *93*, 14474–14479.
- (33) Warshel, A.; Papazyan, A.; Kollman, O. A. *Science* **1995**, *269*, 102–105.
- (34) Koga, K.; Zeng, X. C. *Phys. Rev. Lett.* **1997**, *79*, 853–858.
- (35) Hoh, J. H.; Cleveland, J. P.; Prater, C. B.; Revel, J.-P.; Hansma, P. K. *J. Am. Chem. Soc.* **1992**, *114*, 4917–4922.
- (36) O'Shea, S. J.; Welland, M. E.; Rayment, T. *Appl. Phys. Lett.* **1992**, *60*, 2356–2359.
- (37) Benyon, R. J.; Easterby, J. *The Basics—Buffer Solutions*; IRL Press: London, 1996.
- (38) Zhang, J.; Kirkham, J.; Robinson, C.; Wallwork, M. L.; Smith, D. A.; Marsh, A.; Wong, M. *Anal. Chem.*, in press.
- (39) Wagner, P.; Hegner, M.; Guntherodt, H. J.; G., S. *Langmuir* **1995**, *11*, 3867–3875.
- (40) Hutter, J.; Bechhoefer, J. *Rev. Sci. Instruments* **1993**, *64*, 1868–1872.
- (41) Caspers, J.; Goormaghtigh, E.; Ferreira, J.; Brasseur, R.; Vandenberg, M.; Ruysschaert, J.-M. *J. Colloid Interface Sci.* **1983**, *91*, 546–553.
- (42) Smith, C. P.; White, H. S. *Langmuir* **1993**, *9*, 1–6.
- (43) Holmes-Farley, S. R.; Bain, C. D.; Whitesides, G. M. *Langmuir* **1988**, *4*, 921.
- (44) Crooks, R. M.; Sun, L.; Xu, C.; Hill, S. L.; Ricco, A. J. *Spectroscopy* **1993**, *8*, 28–33.
- (45) van der Vegte, E. W.; Hadziioannou, G. *Langmuir* **1997**, *13*, 4357–4368.
- (46) Yang, H. C.; Dermody, D. L.; Xu, C.; Ricco, A. J.; Crooks, R. M. *Langmuir* **1996**, *12*, 726–735.
- (47) Hall, R. A.; Hayes, D.; Thistlethwaite, P. J.; Grieser, F. *Colloids Surf.* **1991**, *56*, 339–356.
- (48) Lovelock, B.; Grieser, F.; Healy, T. W. *J. Phys. Chem.* **1985**, *89*, 501–507.
- (49) Schrader, M. E. *J. Colloid Interface Sci.* **1984**, *100*, 372–378.
- (50) Rabinovich, Y. I.; Churaev, N. V. *Russ. J. Phys. Chem.* **1990**, *52*, 256–263.
- (51) Kane, V.; Mulvaney, P. *Langmuir* **1998**, *14*, 3303–3311.
- (52) Kokkoli, E.; Zukoski, C. F. *Langmuir* **1998**, *14*, 1189–1195.
- (53) Johnson, K. L.; Kendall, K.; Roberts, A. D. *Proc. R. Soc. London A* **1971**, *324*, 301–313.
- (54) Bouma, W. J.; Radom, L. *Chem. Phys. Lett.* **1979**, *64*, 216–222.
- (55) Emsley, J.; Overill, R. E. *Chem. Phys. Lett.* **1979**, *65*, 616–623.
- (56) Shan, S.-O.; Loh, S.; Herschlag, D. *Science* **1996**, *272*, 97–101.
- (57) Ho, R.; Yuan, J.-Y.; Shao, Z. *Biophys. J.* **1998**, *75*, 1076–1083.
- (58) Liu, G.; Salmeron, M. B.; *Langmuir*, **1994**, *10*, 367–372.
- (59) Holmes-Farley, S. R.; Reamey, R. H.; McCarthy, T. J.; Deutch, J.; Whitesides, G. M. *Langmuir* **1985**, *1*, 725–740.
- (60) Moore, A.; Williams, P. M.; Pope, L.; Davies, M. C.; Roberts, C. J.; Tendler, S. J. B. *J. Chem. Soc., Perkin Trans. 2* **1999**, *200*, 5–8.